

STRUCTURAL ANALYSIS OF A QUASI-RANDOM MASONRY WALL: GEOMETRY DETAILS, HOMOGENIZATION AND APPLICATION

P.B. Lourenço¹, Y. Esquivel² and G. Milani³

¹ Professor, ISISE, University of Minho, Department of Civil Engineering, Azurém, 4800-058 Guimarães, Portugal.
pbl@civil.uminho.pt

² MSc Student, ISISE, University of Minho, Department of Civil Engineering, Azurém, 4800-058 Guimarães,
Portugal. yesquivel@pucp.pe

³ Assistant Professor, Dipartimento di Ingegneria Strutturale (DIS), Politecnico di Milano, Piazza Leonardo da Vinci
32, 20133 Milano, Italy. milani@stru.polimi.it

ABSTRACT

In many countries, historical buildings were built with masonry walls constituted by random assemblages of blocks and stones of variable dimensions. The analysis of historic masonry structures requires often complex and expensive computational tools that in many cases are difficult to handle, given this condition of large variability of masonry. The present paper addresses a methodology for the characterization of the response of rubble masonry. First, a brief state of the art regarding homogenization is presented. Then, the characterization of the masonry and statistical analysis of the dimensions of the stone units from the walls of Guimarães castle are carried out. This is followed by the homogenized limit analysis of representative volume elements (RVEs) from the Alcaçova wall in the Guimarães castle, in order to obtain its in-plane and out-of-plane failure surfaces at different orientations of a load and increasing compressive loads considering the case of masonry with weak and strong mortar independently. Finally, a safety for seismic loading was carried out in two numerical models of the Alcaçova wall, being the first one built with a heterogeneous material and the second one with a homogeneous material that was obtained by means of homogenized limit analysis of representative volume elements. The purpose is to determinate the reliability of results, in terms of limit load and failure mechanism, from the homogenized model, compared to the heterogeneous model.

KEYWORDS: micro-modelling, homogenization techniques, quasi-periodic masonry, geometrical survey, limit analysis, structural safety

INTRODUCTION

Masonry is a common material in many historical buildings around the world. These buildings might have survived seismic events throughout their existence, or might have not experienced an earthquake in the past, but these facts do not mean historical buildings are out of danger. Nowadays, there are powerful analysis tools that allow to model and calculate the safety of complex structures with reasonable approximation. Still, structural analysis of historical masonry buildings remains a challenge due to the low tensile strength of masonry and its quasi-brittle failure, the heterogeneity found and the influence of the bond, among other factors. This increases the computational cost and complicates the numerical models. In recent years, the interest in the conservation of historical buildings and in finding efficient numerical models, has led to a significant number of numerical model for historical masonry buildings, from very simple to complex ones, which are able to simulate the behaviour of the material under different

type of loads. The choice depends on the degree of accuracy, sought in the analysis for each particular case, e.g. [1,2].

This paper concerns the characterization of the response of quasi-periodic masonry by means of a geometrical study and a statistical analysis of stone units, homogenization of masonry and structural implementation. For this purpose, it was decided: (a) to carry out the geometrical investigation of stones units from Guimarães castle to obtain statistical parameters and distribution of the height and length of the stones units, with the aim of determining the adequate size of the representative volume elements; (b) to perform the homogenized limit analysis of representative volume elements (RVEs) to obtain their in-plane failure surfaces and out-of-plane failure surfaces; (c) to carry out the limit analysis of the Alcaçova wall and to compare the limit load and failure mechanisms from the homogeneous model and from the heterogeneous model, in order to check the reliability of the homogenous model.

MASONRY HOMOGENIZATION: A BRIEF STATE-OF-THE-ART

Composite materials are made by two or more different constituents bond by an interface. They can be easily recognised as heterogeneous, such as masonry (composed of stones or bricks in a matrix of mortar), laminated wood, cracked media and porous media, or as homogenous, such as metals and concrete, for which aggregates, matrix or crystals can be more or less recognizable. In the case of masonry a random or structured distribution of their components controls the behaviour. This problem is faced up by a numerical representation that can focus on the micro-modelling of its components (units and mortar) or macro-modelling as a composite [3]. According to the level of accuracy and complexity to be achieved, it is possible to choose the modelling strategies shown in Figure 1.

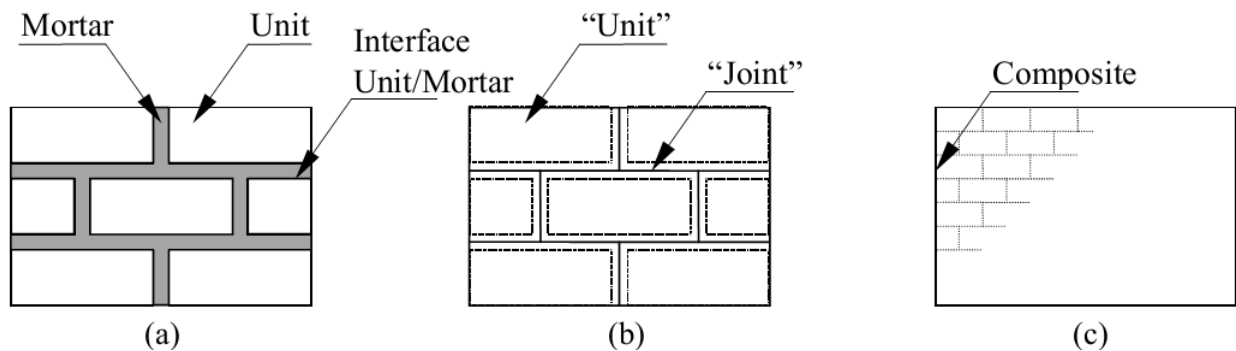


Figure 1: Modelling Strategies for Masonry Structures: a) Detailed Micro-Modelling; b) Simplified Micro-Modelling; c) Macro-Modelling

Another possibility is to adopt homogenization techniques, which consist of choosing a Representative Volume Element (RVE) from the microscopic structure that considers the effect that the microscopic structure causes on the macroscopic behaviour, see [4] for a review. An entire wall can be represented by the repetition of a RVE (or basic cell) that is usually composed by unit, bed joint, head joint and cross joint. Therefore, two scales are considered, microscopic scale, which is small enough to represent the microstructure of masonry, and macroscopic scale, which is larger enough to represent the behaviour of the composite structure (Figure 2).

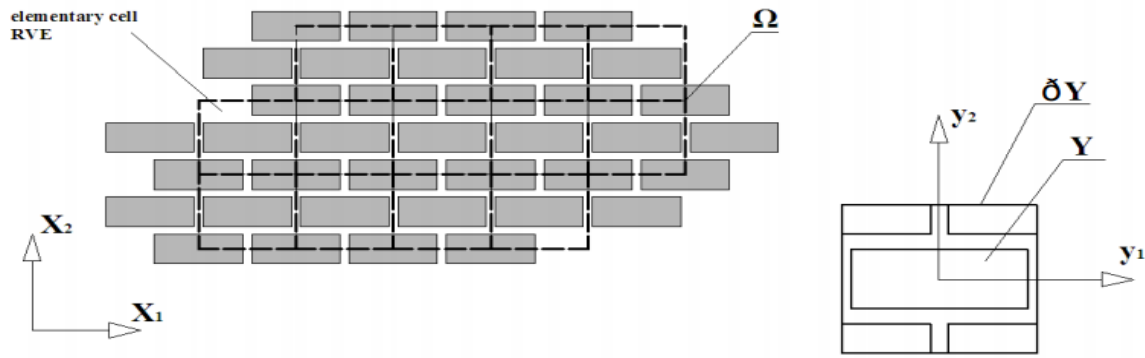


Figure 2: Basic Cell for Masonry Homogenization: Macro- “X” and Micro-Scale “y”

GUIMARÃES CASTLE: GEOMETRY OF THE MASONRY UNITS

The origin of the castle dates back to the 10th century and the fights against the Moors in the Iberian Peninsula. In the 11th century, the first King of Portugal was born there. Later, between the 12th and 14th centuries, the castle was enlarged and the defence capacity was improved. At a certain stage, the castle was abandoned and suffered damage caused by time, and by the subsequent changes of use. In the 20th century, important restoration works have been carried out. The current condition is shown in Figure 3, where the pentagonal plan view of the castle is identified. The castle is surrounded by eight square towers, which delimit the main square, with a main tower (“Torre de Menagem” in Portuguese and “Keep” in English) in the centre. The main wall under study in this paper is the so-called “Alcáçova” Wall, which is originally the highest and most protected part of an Iberian medieval castle, with a defence function and where the civil or ecclesiastical authorities lived. The word was later used to define the part of the castle where the governor lived.

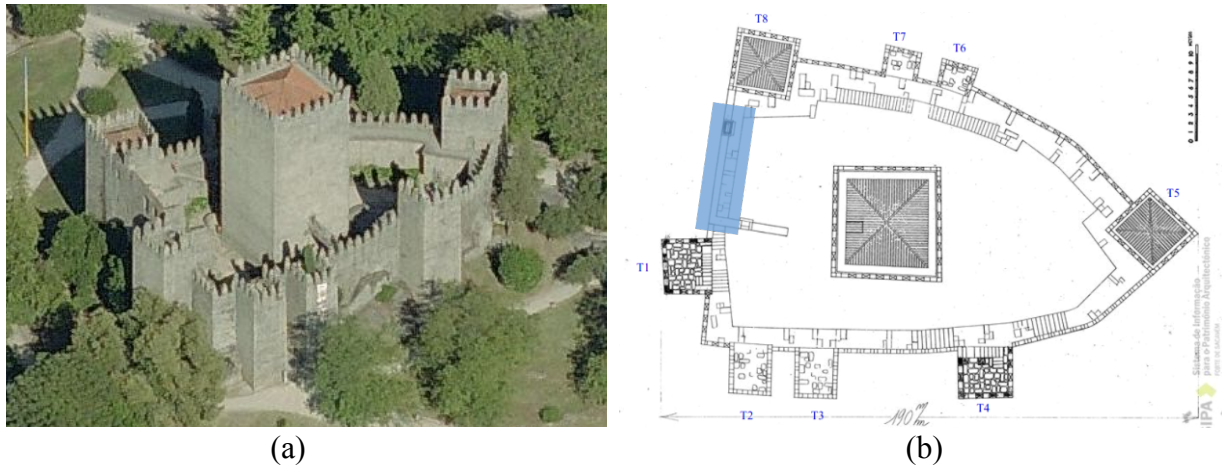


Figure 3: Castle of Guimarães: a) Panoramic View; b) Plan (“Alcáçova” Wall Shaded)

The masonry of the castle is made using granite stone ashlar in the external leaves. The masonry features horizontal courses and is relatively regular, despite the fact that the height of the courses is not constant and that the length of the units is rather variable. In order to represent this feature, a statistical description considering mean, standard deviation, coefficient of variation and probability distribution of the size of the stone units from four walls was made: Wall1, Wall2, Tower wall and Alcáçova wall, see Figure 4. The walls were analysed separately and together as

a single group. The objective was to characterize the length l and height h of stone units and the results are shown in Table 1. The procedure was to identify the stone units in a first step and then to define the best fit probabilistic distribution, which is a lognormal (skew) distribution for both variables.

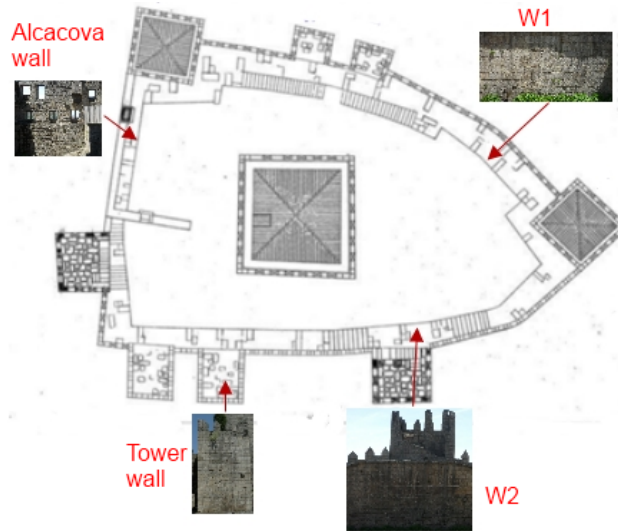


Figure 4: Location of the Wall 1 (W1), Wall 2 (W2), Tower Wall and Alcaçova Wall

Table 1: Geometric Data Measured

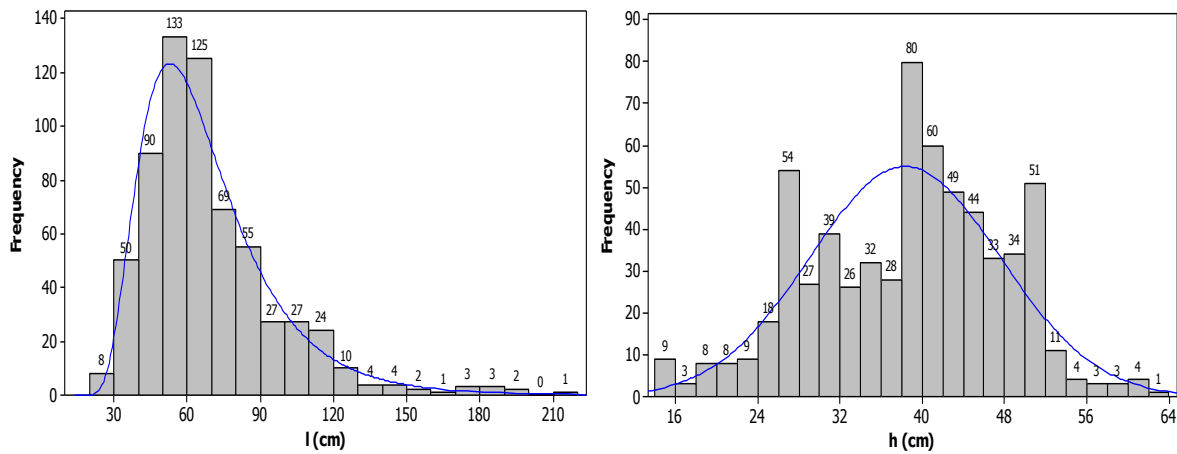
Results Wall	Number of units	Ratio Height / Length h/l	Length			Height		
			Average [m] (CoV)	Typical [m] (Frequency)	Range [m]	Height [m] (CoV)	Typical [m] (Frequency)	Range [m]
Wall W1	110	0.51	0.76 (34%)	0.70 (27%)	0.40-1.70	0.39 (20%)	0.40 (38%)	0.20-0.40
Wall W2	110	0.63	0.70 (27%)	0.65 (27%)	0.45-1.35	0.44 (19%)	0.40 (25%)	0.25-0.60
Tower	110	0.54	0.85 (37%)	0.65 (34%)	0.50-1.80	0.46 (17%)	0.50 (35%)	0.15-0.60
Alcaçova	308	0.56	0.60 (44%)	0.45 (25%)	0.25-2.10	0.34 (23%)	0.40 (35%)	0.15-0.60
Full Sample	Weighted average	0.56	0.69 (40%)	0.55 / 0.65 (21%)/(20%)	0.25-2.10	0.38 (24%)	0.40 (35%)	0.15-0.60

The following aspects from the geometric data are relevant: (a) there is a large variation between the mean value of the stone length and height in the four walls selected for sampling (0.60 to 0.85 m in length and 0.34 to 0.46 m in height). The ratio between the maximum and minimum averages in the different samples is similar in length and height (about 75%); (b) the stone geometrical ratio is rather important for the quality of the masonry bond. The value of h/l for the average geometrical dimensions is about 56% (1:1.8). Only in Wall2, a slightly different h/l ratio

is found, equal to 63% (1:1.6); (c) the scatter found in the length is always much larger than the scatter found in the height, being the scatter in the full sample not so much different from the scatter in the individual samples; (d) wall 2 is the sample with the lowest scatter and the Alcaçova is the sample with the largest scatter, despite the fact that the Alcaçova sample is three times larger than Wall 2; (e) the difference between averaging the total sample weighted by the number of samples or weighted equally is only moderate, with about 5% change in the dimensions; (f) the probabilistic distribution for the length is clearly skewed, requiring a lognormal distribution. The probabilistic distribution for the height is symmetric, meaning that a normal distribution can be used.



(a)



(b)

Figure 5: Geometric Survey of the Units: (a) Identification in the Alcaçova Wall; (b) Distribution of Length (l) and Height (h) in the Entire Sample

HOMOGENIZED LIMIT ANALYSIS OF RVES

Next, a study on different representative volume element (RVE) samples from the Alcaçova wall is presented. The RVEs are analysed under in-plane load in order to obtain the in-plane surface failure at different orientations of a load with respect to the bed joint, considering masonry with

weak and strong mortar joints, aiming at representing a possible injection intervention. The RVEs are also analysed under out-of-plane load in order to obtain the out-of-plane surface failure at increasing compressive loads. The result allows subsequent implementation of the obtained failure surfaces in the study of the full masonry wall. In-plane failure surfaces are described by horizontal strength (σ_h) and vertical strength (σ_v). Out-of-plane failure surfaces are described by horizontal bending moment (M_{11}), vertical bending moment (M_{22}) and torsional moment, or torsion (M_{12}).

The Alcáçova wall is built using two external leaves with an average thickness of 400mm, separated by an infill. It was decided to consider three RVEs of different size: the first size, called 3x3, has dimensions three times the mean width and the mean height of stone; the second size, called 4x4, is four times the mean width and the mean height of stone; and the third size, called 5x5, is fifth times the mean width and the mean height of stone. For each size of RVE, three different samples located randomly on the wall are taken into account, see Figure 6 for an example. Also, three artificial RVEs were built using mean size stones and periodic arrangement in order to compare the failure surfaces between the RVEs with quasi periodic arrangement and the RVEs with periodic arrangement using average geometry. A linearized Lourenço and Rots [5] failure criterion is adopted for joints reduced to interfaces and a classic Mohr-Coulomb failure criterion is used for brick interfaces, as in [6,7].



Figure 6: Location of 3x3 Representative Volume Elements (RVEs)

The in-plane homogenized failure surfaces ($\sigma_v - \sigma_h$) are obtained keeping a ϑ angle fixed. This angle measures the rotation of the principal stresses with respect to the material axes. Three different ϑ angles are considered $\vartheta=0^\circ$, $\vartheta=22.5^\circ$ and $\vartheta=45^\circ$ (Figure 7a) in analogy to [8]. For each RVE and in each orientation ϑ , 32 values with steps of half of 22.5° have been calculated. The 32 points were then connected to draw failure surfaces. The optimization problem arising in order to obtain the failure surface is solved by using an algorithm code developed in [9]. For masonry with weak mortar, the compressive strength of masonry is assumed equal to 12 MPa and the ultimate tensile strength of joints is assumed equal to 0.05 MPa. The compressive strength of stones is assumed equal to 89.5 MPa and their ultimate tensile strength is equal to 0.93 MPa [10]. For masonry with strong mortar, only the ultimate tensile strength of masonry is changed, assuming a value equal to 0.3 MPa.

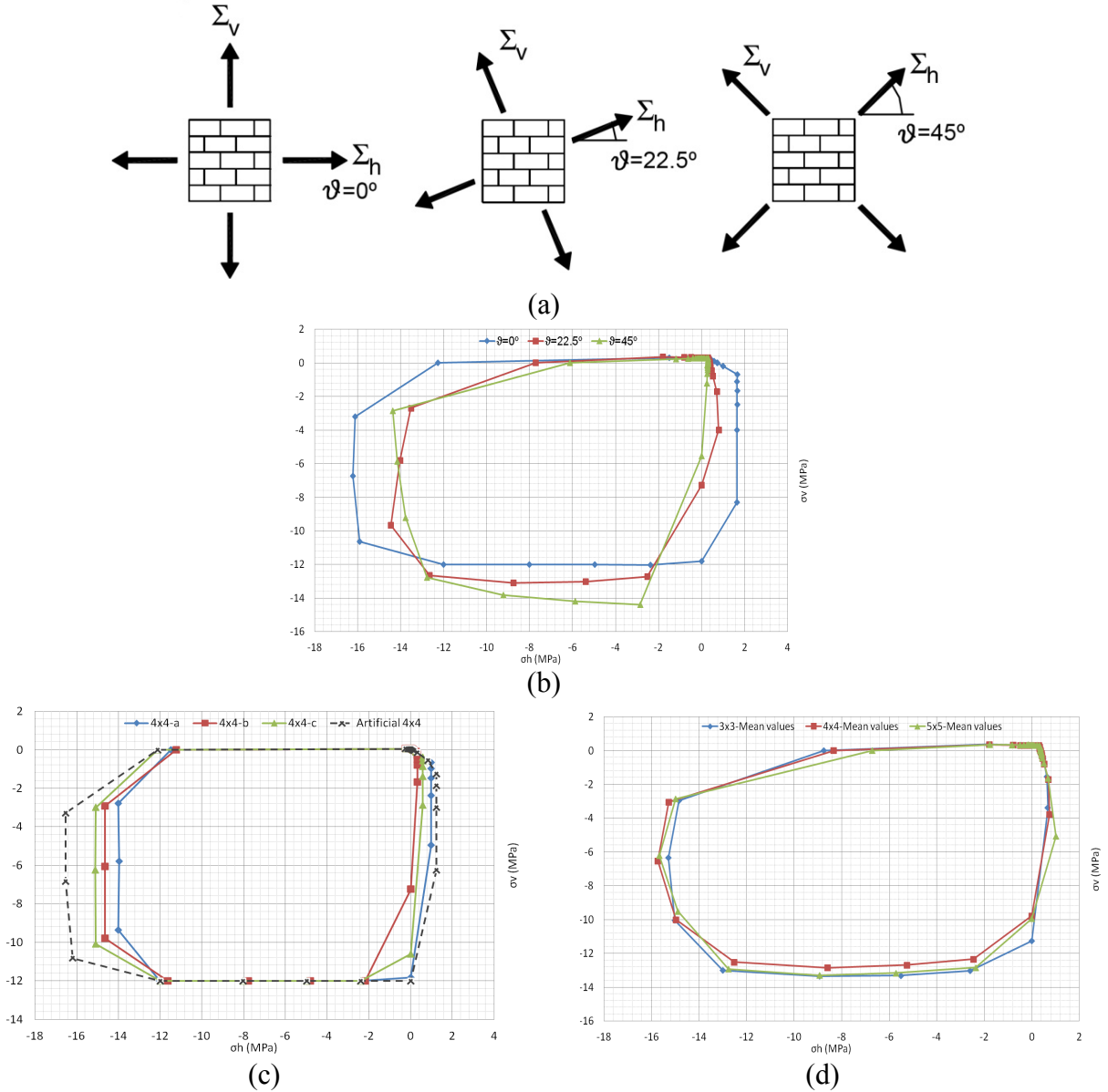


Figure 7: Homogenization: (a) ϑ Angle Orientations of the External Load with Respect to the Bed Joint; (b) Example of a Result with Different Orientations; (c) Example of a Result for Different Cells of the Same Size; (d) Example of a Result for Cells of Different Size.

Figure 7b shows typical in-plane homogenized failure surfaces for RVEs of masonry with weak mortar at different orientations of the load with respect to the bed joint. The usual anisotropic behaviour of masonry is found. Figure 7c shows a comparison between in-plane homogenized failure surfaces obtained from RVEs of the same size and artificial RVEs with periodic arrangement for masonry at a given orientation. Finally, Figure 7d shows a comparison between the mean values of in-plane homogenized failure surfaces at a given orientation for all sizes of the RVEs, where it is shown that small difference are found. These results seem to indicate that the average of 3 masonry samples, with minimum size of 3x3, provides a reasonable estimate of the true failure surface. Further details on these results can be found in [11].

Failure modes obtained from representative volume elements are depicted in Figure 8, where a qualitative comparison with experimental results [12] is also shown. A staircase crack in the 4x4 representative volume element is found independently of the quality of the mortar. It is noted that dilatancy is present in the numerical model, even if it is believed that the influence in the global behaviour is very low (the upper boundary is allowed to move up, meaning that an artificial confining stress built up does not occur).

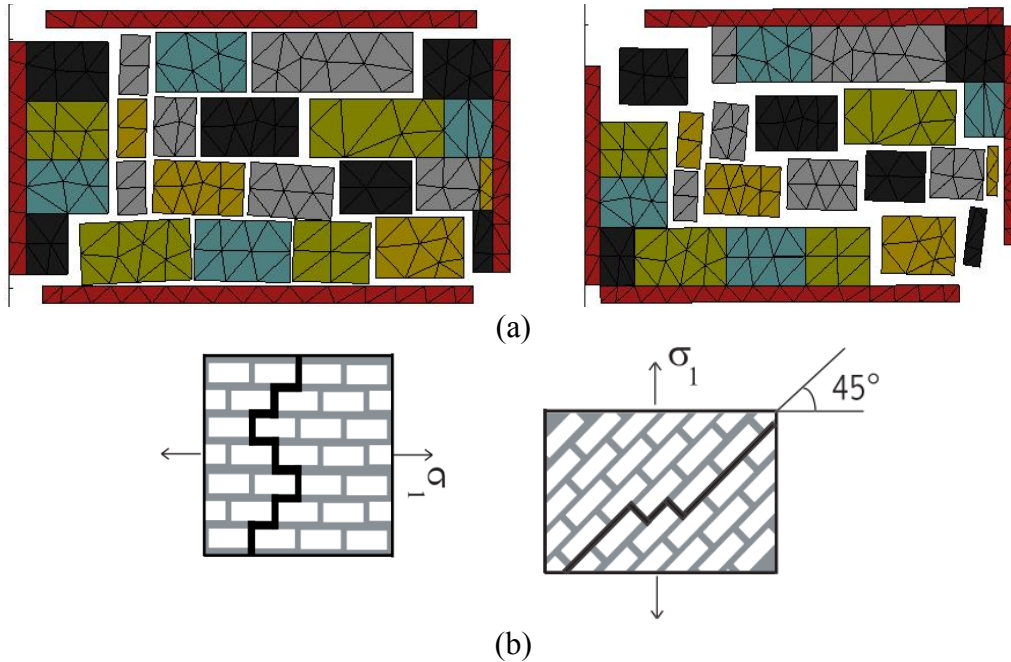


Figure 8: Qualitative Comparison of Mode Failure Between a Masonry RVE with Load Orientations Equal to $\theta=0^\circ$ and 45° : (a) Numerical; (b) Experimental [12].

OUT-OF-PLANE HOMOGENIZED FAILURE SURFACES

As post-earthquake surveys have shown out-of-plane loading causes the main failures and damage in masonry structures, and especially in historical buildings, whose façades are usually characterized by a relative small thickness in comparison with height and length. For this reason it is important to carry out a study about homogenized out-of-plane failure surfaces (M_{11} - M_{22} and M_{11} - M_{12}) which are obtained from a combination of homogenization techniques and limit analysis. Again, plasticity and associated flow rule for the constituent materials are assumed. The RVE is subdivided into 12 layers along the thickness (a conservative thickness is considered, assuming only the Alcaçova wall external leaf, with $h = 400$ mm). For each layer, the out-of-plane components σ_{i3} ($i=1, 2, 3$) of the micro-stress tensor σ are set to zero, meaning that only the in-plane components σ_{ij} ($i,j=1,2$) are considered active and constant in the thickness.

The out-of-plane homogenized failure surfaces in sections in the space of bending moment (M_{22}) and horizontal bending moment (M_{11}) are generated from the integration of in-plane homogenized stress for which the algorithm requires the following data: The thickness of the RVE, assumed as 0.40m; the number of layers in which the thickness of the RVE will be divided, selected as twelve layers; the compressive vertical load, which is considered at three different levels $N_{22}=0$ (top), $N_{22}=\text{self-weight}/2$ (mid-height), $N_{22}=\text{self-weight}$ (bottom) of the Alcaçova wall; and the values of the in-plane failure surfaces. On the other hand for obtaining

the out-of-plane homogenized failure surfaces in sections in the space of torsion (M_{12}) and horizontal bending moment (M_{11}), the algorithm requests the geometry of the mesh, number of elements and the properties of the masonry, using a process similar to the case of in-plane loads.

Figure 9a shows out-of-plane homogenized failure surfaces (M_{11} - M_{22}) for RVEs with increasing vertical compressive loads. As it can be seen, the vertical compression applied increases not only the horizontal bending moment (M_{11}) but also the vertical bending (M_{22}) and torsion (M_{12}). This means that bed joints, in general, contribute to masonry vertical and torsion ultimate moment due to the friction effect of interlocking units. In some cases, due to insufficient staggering of the stones in the RVE with strong mortar, M_{11} does not increase as a straight vertical crack is obtained. Figure 9b shows out-of-plane homogenized failure surfaces (M_{11} - M_{12}) for RVEs of masonry with increasing vertical compressive loads. Again, the vertical compression load applied usually increases not only the horizontal bending moment but also the vertical bending moment (M_{11}) and torsion (M_{12}). Finally, Figure 9c shows a comparison between the mean values of out-of-plane homogenized failure surfaces of RVEs of the same size when the compressive load is maximum, $N_{22}=133$ kN/m. As it can be observed, the vertical bending moment (M_{22}) exhibits similar values for the different cell sizes (as well as the torsion M_{12} [11]). The horizontal bending moment (M_{11}) exhibits some scatter for the different average results, as it is more sensitive to the compressive loads. Still, the scatter is moderate for engineering purposes.

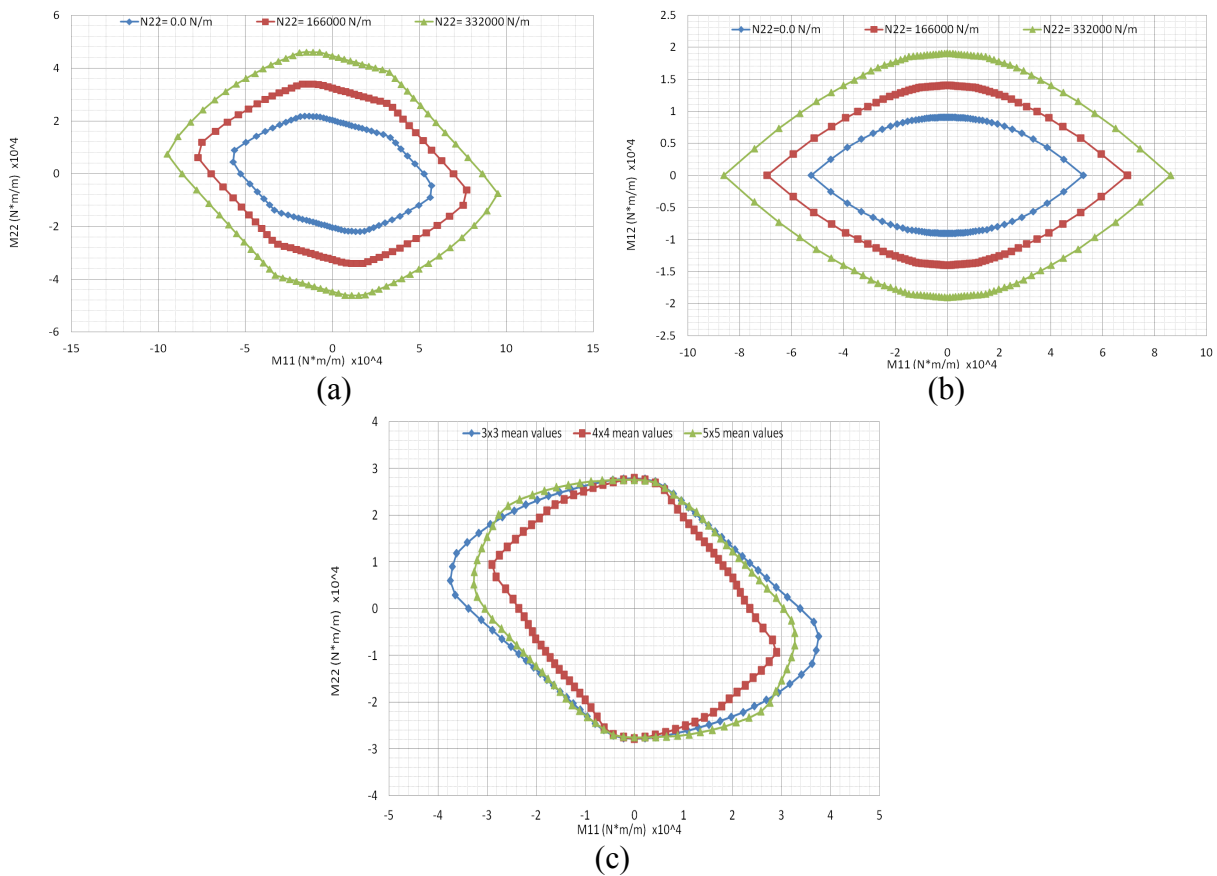


Figure 9: Results of Out-of-Plane Homogenization: Example of Failure Surfaces in (a) $(M_{11}-M_{22})$ Plane and in (b) $(M_{11}-M_{12})$ Plane for Increasing Vertical Compression; (c) Comparison Between the Mean Values for Different RVEs Sizes.

LIMIT ANALYSIS OF THE ALCAÇOVA WALL OF GUIMARÃES CASTLE

The present study is focused in the part of the Alcaçova wall located above a much thicker wall part, composed by two external leaves of stone masonry and an infill material in the middle. This wall is supported on three edges, in the base of the wall, left side and right side. The dimensions of the wall are 14.2 m length, 6.9 m height and 0.40 m thickness for each leaf [11]. The wall has six openings that represent approximately 20% of the area of the entire wall. Above each opening, a lintel is present. In order to carry out the analysis of Alcaçova wall, two numerical models are developed, only for the (weaker and thinner) upper part of the wall. The first model considered is a homogeneous numerical model composed by a mesh of 173 triangular elements and 127 nodes, whereas the second model is a heterogeneous model built considering the existing arrangement of stones, 308 unit stones in total, and mortar joints reduced to interfaces, as the thickness of the mortar joints is much smaller than the dimension of stones. This model is composed by a mesh of 1299 triangular elements and 740 nodes.

Two hypotheses are considered for the masonry. In the first case (weak mortar, representing the actual condition), the tensile strength of stones is equal to 0.93N/mm^2 , the tensile strength and cohesion of mortar joints reduced to interfaces are 0.05 N/mm^2 and 0.05 N/mm^2 , respectively. In a second case (strong mortar, representing the behaviour after injection), the tensile strength of stones remains equal, but the tensile strength and cohesion of mortar joints reduced to interfaces are 0.3 N/mm^2 and 0.45 N/mm^2 , respectively. The input of material data for the homogeneous model are the out-of-plane failure surfaces obtained from the analysis of the representative volume element, which are assigned according the different values of the vertical load along the height of the Alcaçova wall.

The results of non-linear limit analysis show the limit load and the possible collapse mechanisms of the Alcaçova wall under out-of-plane loads, which can be caused by a seismic action. It is worth to note that limit analysis does not provide information related with displacements. The possible mechanisms are identified taking into account the cracks patterns. The results, obtained from the numerical homogenous model and numerical heterogeneous model are compared in order to know how accurate and reliable the homogeneous model is.

Figure 10 shows typical failure mechanisms of the analyses, where it is shown that there is reasonable agreement between homogenous and heterogeneous model. The limit analysis load of the heterogeneous model with weak mortar equals 8.9% of the self-weight and the limit load of the homogeneous model is equal to 6.9% of the self-weight, which are again in reasonable agreement (20% difference). The limit load of the heterogeneous model with strong mortar is equal to 34% of the self-weight, whereas the limit load of the homogeneous model is equal to 32% of the self-weight, again in reasonable agreement (10% difference). It is also interesting to observe that the introduction of strong mortar significantly increases the limit load of the Alcaçova wall (almost four times).

Finally, it is noted that the analysis was performed on a standard PC Intel Pentium Dual 2.12 GHz equipped with 3GB RAM. A comparison in terms of processing time, only for computing, indicates that the homogeneous model saves about 95% calculation time (30 vs. 600 seconds) and mesh preparation times (three vs. sixteen hours).

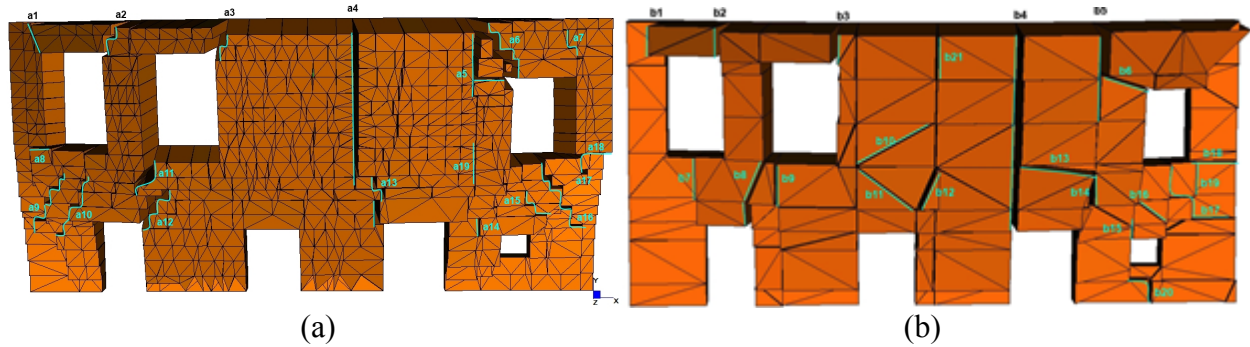


Figure 10: Typical Wall Collapse: (a) Heterogeneous and (b) Homogenous Model.

CONCLUSIONS

Non-linear tools often imply expensive computational costs, a good knowledge about non-linear processes and a large time to build the model and perform the analysis. This problem was addressed here by means of a geometrical investigation and homogenization of masonry. The limit analysis of the Alcaçova wall of Guimarães castle is carried out by means of two models, heterogeneous and homogenized material. The homogeneous model provides good agreement with the heterogeneous model, in terms of failure load and mechanism, at a fraction of the cost.

REFERENCES

1. Lourenço, P.B., Mendes, N., Ramos, L.F., Oliveira, D.V. (2011) "Analysis of masonry structures without box behavior" *International Journal Architectural Heritage*, 5, p. 369-382.
2. Lourenço, P.B. (2002) "Computations of historical masonry constructions" *Progress in Structural Engineering and Materials*, 4(3), p. 301-319.
3. J.G. Rots (1991) "Numerical simulation of cracking in structural masonry" *Heron*, 36(2), p. 49-63.
4. Lourenço, P.B., Milani, G., Tralli, A., Zucchini, A. (2007) "Analysis of masonry structures: review of and recent trends of homogenisation techniques" *Canadian Journal of Civil Engineering*, 34 (11), p. 1443-1457.
5. Lourenço, P.B., Rots, J.G. (1997) "Multisurface interface model for the analysis of masonry structures" *J. Engrg. Mech., ASCE*, 123(7), p. 660-668.
6. Milani, G., Lourenço, P.B., Tralli, A. (2006) "Homogenised limit analysis of masonry walls, Part I: failure surfaces" *Computers & Structures*, 84, p. 166-180.
7. Sutcliffe, D.J., Yu, H.S., Page, A.W. (2001) "Lower bound limit analysis of unreinforced masonry shear walls" *Computers & Structures*, 79, p. 1295-312.
8. Page, A.W. (1987) "Biaxial failure criterion for brick masonry in the tension-tension range" *International Masonry Journal*, 1, p. 26-30.
9. Milani, G., Lourenço, P.B. (2010) "Monte Carlo homogenized limit analysis model for randomly assembled blocks in-plane loaded" *Computational Mechanics*, 46(6), p. 827-849.
10. Vasconcelos, G., Lourenço, P.B., Alves C.A.S., Pamplona, J. (2008) "Experimental characterization of the tensile behaviour of granites" *International Journal of Rock Mechanics and Mining Sciences*, 45(2), 268-277.
11. Esquivel, Y. (2012) "Characterization of the response of quasi-periodic masonry", MSC Thesis, University of Minho. Available from <http://www.msc-sahc.org/>.
12. Dhanasekar, M., Page, A.W., Kleeman, P.W. (1985) "The failure of brick masonry under biaxial stresses" *Proc. Instn. Civ. Engrs., Part 2*, 79(2), p. 295-313.